1. INTRODUCTION

Recently flow problems in porous tubes or channels have been under considerable attention because of its various applications in biomedical engineering, for example, the dialysis of blood in artificial kidney [1], the flow of blood in the capillaries [2], the flow in blood oxygenators [3], and many other engineering areas such as the design of filters [4], transpiration cooling boundary layer control [5] and gaseous diffusion [6]. In 1953, Berman [7] described an exact solution of the Navier-Stokes equation for steady two-dimensional laminar flow of a viscous, incompressible fluid in a channel with parallel rigid porous walls driven by uniform, steady suction or injection at the walls. This mass transfer is paramount in some industrial processes. Lately, Chandran and Sacheti [8] analyzed the effects of a magnetic field on the thermodynamic flow past a continuously moving porous plate. In fluid mechanics, many of the problems end up to a complicated set of nonlinear ordinary differential equations which can be solved using different analytic method, such as homotopy perturbation method, variational iteration method introduced by He [9].

The homotopy perturbation method, proposed first by He in 1998 and was further developed and improved by He [10]. It yields a very rapid convergence of the solution series in most cases. Sheikholeslami et al. [11] applied this method to investigate Hydromagnetic flow between two horizontal plates in a rotating system. They reported that increasing magnetic parameter or viscosity parameter leads to decreasing Nu. By increasing the rotation parameter, blowing velocity parameter and Pr the Nusselt number increases. Sheikholeslami et al. [12] studied the three-dimensional problem of steady fluid deposition on an inclined rotating disk using HPM. They concluded that by increasing normalized thickness, Nusselt number increases. However, this trend is more noticeable in grater Prandtl numbers.

Considered Fluid heating and cooling are important in many industries such as power, manufacturing and transportation. Effective cooling techniques are absolutely necessary for cooling any sort of high energy device. Common heat transfer fluids such as water, ethylene glycol, and engine oil have limited heat transfer capabilities due to their low heat transfer properties.

In contrast, thermal conductivity of metals are up to three times higher than those of fluids. Therefore, it is naturally desirable to combine the two substances to produce a heat transfer medium that behaves like a fluid, but has the thermal conductivity of a metal. Recently, several studies have been carried out on nanofluids. Steady magnetohydrodynamic free convection boundary layer flow past a vertical semi-infinite flat plate embedded in water filled with a nanofluid has been theoretically studied by Hamad et al. [13]. They have found that Cu and Ag nanoparticles proved to have the highest cooling performance for this problem.

Soleimani et al. [14] studied natural convection heat transfer in a semi-annulus enclosure filled with nanofluid using the Control Volume based Finite Element Method. Also, it is reported that the angle of turn has an important effect on the streamlines, isotherms and maximum or minimum values of local Nusselt number.

Sheikholeslami et al. [15] have investigated the flow of nanofluid and heat transfer characteristics between two horizontal plates in a rotating system. Their results show that for suction and injection, the heat transfer rate at the surface increases by increasing the nanoparticle volume fraction, Reynolds number, and injection/suction parameter and it decreases with power of rotation parameter. Natural convection of a non-Newtonian copper-water nanofluid between two infinite parallel vertical flat plates has been investigated by Domairry et al. [16].

They have concluded that as the volume fraction of nanoparticle increases, the momentum boundary layer thickness increases, while the thermal boundary layer thickness decreases. Sheikholeslami et al. [17] studied the natural convection in a concentric annulus between a cold outer square and heated inner circular cylinders in presence of static radial magnetic field. They have reported that average Nusselt number is an increasing function of nanoparticle volume fraction as well as Rayleigh number, while it is a decreasing function of Hartmann number.

Sheikholeslami et al. [18] performed a numerical analysis for natural convection heat transfer of Cu-water nanofluid in a cold outer circular enclosure containing a hot inner sinusoidal circular cylinder in presence of horizontal magnetic field using the Control Volume based Finite Element Method. They have induced that in absence of magnetic field, enhancement ratio decreases as Rayleigh number increases; while in presence of magnetic field an opposite trend, was observed. Sheikholeslami et al. [19] studied the effects of magnetic field and nanoparticle on the Jeffery-Hamel flow by ADM. They have shown that increasing Hartmann number will lead to backflow reduction. In greater angles or higher Reynolds numbers, high Hartmann number is needed to reduce the backflow. Also, the results show that momentum boundary layer thickness causes increase of nanoparticle volume fraction. The main aim is to investigate the problem of laminar nanofluid flow in a semi-porous channel in the presence of transverse magnetic field using Homotopy Perturbation Method. The effects of the nanofluid volume friction, Hartmann number and Reynolds number on velocity profile are considered.

2. MATHEMATICAL MODEL

Consider the laminar two-dimensional stationary flow of an electrical conducting incompressible viscous fluid in a semi-porous channel made by a long rectangular plate with length of L_x in uniform translation in x^* direction and an infinite porous plate. The distance between the two plates is h. We observe a normal velocity q on the porous wall. A uniform magnetic field B is assumed to be applied towards direction y^*(Figure 1). In case of a short circuit to neglect the electrical field, perturbations to the basic normal field and without gravity forces, the governing equations are:

$$\frac{\partial u^*}{\partial x^*}+\frac{\partial v^*}{\partial y^*}=0, \tag{1}$$

$$u^*\frac{\partial u^*}{\partial x^*}+v^*\frac{\partial u^*}{\partial y^*}=-\frac{1}{\rho_{nf}}\frac{\partial P^*}{\partial x^*}+\frac{\mu_{nf}}{\rho_{nf}}\left(\frac{\partial^2 u^*}{\partial x^{*2}}+\frac{\partial^2 u^*}{\partial y^{*2}}\right)-u^*\frac{\sigma_{nf}B^2}{\rho_{nf}} \tag{2}$$

$$u^*\frac{\partial v^*}{\partial x^*}+v^*\frac{\partial v^*}{\partial y^*}=-\frac{1}{\rho_{nf}}\frac{\partial P^*}{\partial y^*}+\frac{\mu_{nf}}{\rho_{nf}}\left(\frac{\partial^2 v^*}{\partial x^{*2}}+\frac{\partial^2 v^*}{\partial y^{*2}}\right) \tag{3}$$

The boundary conditions for the velocity are:

$$y^*=0: u^*=u_0^*, v^*=0, \tag{4}$$

$$y^*=h: u^*=0,\ v^*=-q, \tag{5}$$

Calculating a mean velocity U by the relation:

$$y^*=0: u^*=u_0^*, v^*=0, \tag{6}$$

We consider the following transformations:

$$x=\frac{x^*}{L_x};\ y=\frac{y^*}{h}, \tag{7}$$

$$u=\frac{u^*}{U};\ v=\frac{v^*}{q},\ P_y=\frac{P^*}{\rho_f.q^2} \tag{8}$$

Then, we can consider two dimensionless numbers: the Hartman number Ha for the description of magnetic forces [1] and the Reynolds number Re for dynamic forces:

$$Ha=Bh\sqrt{\sigma_f/\rho_f.\upsilon_f}, \tag{9}$$

$$\mathrm{Re}=\frac{hq}{\mu_{nf}}\rho_{nf}. \tag{10}$$

The effective density (ρ_{nf}) is defined as [18]:

$$\rho_{nf}=\rho_f(1-\phi)+\rho_s\phi \tag{11}$$

where ϕ is the solid volume fraction of nanoparticles. The dynamic viscosity of the nanofluids is [20]:

$$\mu_{nf}=\frac{\mu_f}{(1-\phi)^{2.5}} \tag{12}$$

The effective thermal conductivity can be modeled by the Maxwell–Garnetts as [18]:

$$\frac{k_{nf}}{k_f}=\frac{k_s+2k_f-2\phi(k_f-k_s)}{k_s+2k_f+\phi(k_f-k_s)} \tag{13}$$

The effective electrical conductivity of nanofluid was presented by Maxwell [18] as:

$$\frac{\sigma_{nf}}{\sigma_f}=1+\left[3\left(\frac{\sigma_s}{\sigma_f}-1\right)\phi/\left(\left(\frac{\sigma_s}{\sigma_f}+2\right)-\left(\frac{\sigma_s}{\sigma_f}-1\right)\phi\right)\right] \tag{14}$$

The thermo physical properties of the nanofluid are given in Table 1 [18].

So, we can evolve the dimensionless equations:

$$\frac{\partial u}{\partial x}+\frac{\partial v}{\partial y}=0, \tag{15}$$

$$u\frac{\partial u}{\partial x}+v\frac{\partial u}{\partial y}=-\varepsilon^2\frac{\partial P_y}{\partial x}+\frac{\mu_{nf}}{\rho_{nf}}\frac{1}{hq}\left(\varepsilon^2\frac{\partial^2 u}{\partial x^2}+\frac{\partial^2 u}{\partial y^2}\right)-u\frac{Ha^2}{\mathrm{Re}}\frac{B^*}{A^*} \tag{16}$$

$$u\frac{\partial \upsilon}{\partial x}+v\frac{\partial v}{\partial y}=-\frac{\partial P_y}{\partial x}+\frac{\mu_{nf}}{\rho_{nf}}\frac{1}{hq}\left(\varepsilon^2\frac{\partial^2 v}{\partial x^2}+\frac{\partial^2 v}{\partial y^2}\right) \tag{17}$$

where A^* and B^* are constant parameters:

$$A^*=(1-\phi)+\frac{\rho_s}{\rho_f}\phi,$$
$$B^*=1+\left[3\left(\frac{\sigma_s}{\sigma_f}-1\right)\phi/\left(\left(\frac{\sigma_s}{\sigma_f}+2\right)-\left(\frac{\sigma_s}{\sigma_f}-1\right)\phi\right)\right] \tag{18}$$

Quantity of ε is defined as the aspect ratio between distance h and a characteristic length L_x of the slider.

TABLE 1. Thermo physical properties of water and nanoparticles [18].

	Pure water	**Copper (Cu)**
$\rho(kg/m^3)$	997.1	8933
$C_p(j/kgk)$	4179	385
$k(W/m.k)$	0.613	401
$\sigma(\Omega^{-1}m^{-1})$	0.05	5.96×10^7

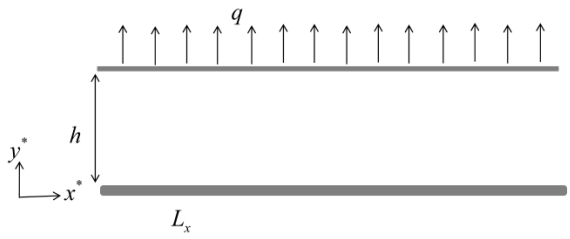

Figure 1. Schematic diagram of the system

It is normally small. Berman's similarity transformation is used to be free from ε:

$$v = -V(y); u = \frac{u^*}{U} = u_0 U(y) + x\frac{dV}{dy}. \quad (19)$$

Introducing Equation (19) in the second momentum Equation (17) shows that quantity $\partial P_y / \partial y$ does not depend on the longitudinal variable x. By first momentum equation, we also observe that $\partial^2 P_y / \partial x^2$ is independent of x. We omit asterisks for simplicity. Then a separation of variables leads to [21]:

$$V'^2 - VV'' - \frac{1}{\mathrm{Re}}\frac{1}{A^*(1-\phi)^{2.5}}V''' + \frac{Ha^2}{\mathrm{Re}}\frac{B^*}{A^*}V' = \varepsilon^2\frac{\partial^2 P_y}{\partial x^2} = \varepsilon^2\frac{1}{x}\frac{\partial P_y}{\partial x} \quad (20)$$

$$UV' - VU' = \frac{1}{\mathrm{Re}}\frac{1}{A^*(1-\phi)^{2.5}}\left[U'' - Ha^2 B^*(1-\phi)^{2.5}U\right] \quad (21)$$

The right-hand side of Equation (20) is constant. By derivation respect to x, we have:

$$V^{IV} = Ha^2 B^*(1-\phi)^{2.5}V'' + \mathrm{Re}\,A^*(1-\phi)^{2.5}\left[V'V'' - VV'''\right] \quad (22)$$

where primes denote differentiation with respect to y and asterisks have been omitted. The dynamic boundary conditions are:

$$y = 0: \; U = 1; V = 0; V' = 0, \quad (23)$$

$$y = 1: \; U = 0; V = 1; V' = 0. \quad (24)$$

3. ANALYSIS OF HOMOTOPY PERTURBATION METHOD

To illustrate the basic ideas of this method, we consider the following equation:

$$A(u) - f(r) = 0 \qquad r \in \Omega \quad (25)$$

With the boundary condition of:

$$B\left(u, \frac{\partial u}{\partial n}\right) = 0, \qquad r \in \Gamma, \quad (26)$$

where A is a general differential operator, B a boundary operator, $f(r)$ a known analytical function and Γ is the boundary of the domain Ω. A can be divided into two parts which are L and N, where L is linear and N is nonlinear. Equation (27) can therefore be rewritten as follows:

$$L(u) + N(u) - f(r) = 0 \qquad r \in \Omega \quad (27)$$

Homotopy perturbation structure is:

$$H(v, p) = (1-p)[L(v) - L(u_0)] + p[A(v) - f(r)] = 0 \quad (28)$$

$$v(r, p): \; \Omega \times [0,1] \to R \quad (29)$$

In Equation (5), $p \in [0, 1]$ is an embedding parameter and u_0 is the first approximation that satisfies the boundary condition. We can assume that the solution of Equation (18) can be written as a power series in p, as following:

$$v = v_0 + pv_1 + p^2 v_2 + \ldots \quad (30)$$

and the best approximation for solution is:

$$u = \lim_{p \to 1} v = v_0 + v_1 + v_2 + \ldots \quad (31)$$

4. IMPLEMENTION OF THE METHOD

According to HPM, we construct a homotopy. Suppose the solution of Equation (28) has the form:

$$H(V, p) = (1-p)\left(V^{IV} - V_0^{IV}\right) + p\left(-V^{IV} + Ha^2 B^*(1-\phi)^{2.5}V'' + Re\,A^*(1-\phi)^{2.5}\left[V'V'' - VV'''\right]\right) = 0 \quad (32)$$

$$H(U, p) = (1-p)(U'' - U_0'') + p\left(-UV' + VU' + \frac{1}{Re}\frac{1}{A^*(1-\phi)^{2.5}}\left[U'' - Ha^2 B^*(1-\phi)^{2.5}U\right]\right) = 0 \quad (33)$$

We consider V and U as follows:

$$V(y) = V_0(y) + V_1(y) + \ldots = \sum_{i=0}^{n} V_i(y) \quad (34)$$

$$U(y) = U_0(y) + U_1(y) + \ldots = \sum_{i=0}^{n} U_i(y) \quad (35)$$

By substituting F from Equations (34) and (35) Equations (32) and (33) into and some simplification and rearranging based on powers of p–terms, according to the boundary conditions, we have:

$$p^0: \; V_0^{iv} = 0, U_0'' = 0, \quad (36)$$

$$p^1: \; -Ha^2(1-\phi)^{-2.5}B^*V_0'' + V_1^{iv} + Re\,A^*(1-\phi)^{-2.5}V_0'''V_0 - Re\,A^*(1-\phi)^{-2.5}V_0''V_0' = 0$$
$$-Ha^2(1-\phi)^{-2.5}B^*U_0'' + U_1'' - Re\,A^*(1-\phi)^{-2.5}V_0'U_0 + Re\,A^*(1-\phi)^{-2.5}V_0U_0' = 0 \quad (37)$$

Solving Equations (36) and (37) with boundary conditions, we have:

$$V_0(y) = -2y^3 + 3y^2, \quad U_0(y) = -y + 1. \quad (38)$$

$$
\begin{aligned}
V_1(y) &= 0.0571428\,Re\,A^*(1-\phi)^{-2.5}\,y^7 \\
&\quad - 0.2\,Re\,A^*(1-\phi)^{-2.5}\,y^6 \\
&\quad - 0.1Ha^2(1-\phi)^{-2.5}\,B^*\,y^5 \\
&\quad + 0.3\,Re\,A^*(1-\phi)^{-2.5}\,y^4 \\
&\quad - 0.385714\,Re\,A^*(1-\phi)^{-2.5}\,y^3 \\
&\quad - 0.2Ha^2(1-\phi)^{-2.5}\,B^*\,y^3 \\
&\quad + 0.22857142\,Re\,A^*(1-\phi)^{-2.5}\,y^2 \\
&\quad + 0.5Ha^2(1-\phi)^{-2.5}\,B^*\,y^2
\end{aligned} \tag{39}
$$

$$
\begin{aligned}
U_1(y) &= -0.2\,Re\,A^*(1-\phi)^{-2.5}\,y^5 \\
&\quad - 0.7\,Re\,A^*(1-\phi)^{-2.5}\,y^4 \\
&\quad - 0.16667Ha^2(1-\phi)^{-2.5}\,B^*y^3 \\
&\quad + 0.1\,Re\,A^*(1-\phi)^{-2.5}\,y^3 + 0.5Ha^2(1-\phi)^{-2.5}\,B^*y^2 \\
&\quad - 0.45\,Re\,A^*(1-\phi)^{-2.5}\,y \\
&\quad - 0.3333Ha^2(1-\phi)^{-2.5}\,B^*y
\end{aligned}
$$

when $i \geq 2$ the terms $V_i(y), U_i(y)$ are too large; that is graphically mentioned. When $p \to 1$, we have the following relations:

$$
\begin{aligned}
V(y) &= V_0(y) + V_1(y) + \ldots = \sum_{i=0}^{n} V_i(y) \\
U(y) &= U_0(y) + U_1(y) + \ldots = \sum_{i=0}^{n} U_i(y)
\end{aligned} \tag{40}
$$

5. RESULTS AND DISCUSSION

In this study homotopy perturbation method is applied to obtain an explicit analytical solution of the laminar nanofluid flow in a semi-porous channel in the presence of uniform magnetic field (Figure 1). The results that obtained by homotopy perturbation method matched well with the results carried out by the numerical solution obtained by four-order Rung-kutte method as shown in Figure 2 and Table 2. The percentage error is:

$$
\%\text{Error} = \frac{\left| f(\eta)_{NM} - f(\eta)_{HPM} \right|}{f(\eta)_{NM}} \times 100 \tag{43}
$$

Figure 2(c) shows the average error for different functions at various iterations. As can be seen in this figure homotopy-perturbation method is converged in step 8 and error has been minimized. The effect of nanoparticle volume fraction on $U(y)$ is shown in Figure 3. For both cases, presence and absence of magnetic field, velocity boundary layer thickness decreases with increase of nanoparticle volume fraction. Also, it can be seen that increasing nanoparticle volume friction leads to decrease the values of $U(y)$ and this decrement is more sensible in absence of magnetic field. Effect of various values of Hartmann numbers on $V(y)$ and $U(y)$ is shown in Figure 4. Generally, when the magnetic field is imposed on the enclosure, the velocity field suppressed owing to the retarding effect of the Lorenz force. For low Reynolds numbers, as Hartmann number increases $V(y)$ decreases for $y > y_m$, but opposite trend is observed for $y > y_m$; y_m is a meeting point that all curves joint together at this point. When Reynolds number increases this meeting point shifts to the solid wall and it can be seen that $V(y)$ decreases with increase of Hartmann number. As Hartmann number increases $U(y)$ decreases for all values of Reynolds number. Besides, this figure shows that this change is more pronounced for low Reynolds number.

TABLE 2. Comparison between numerical results and HPM when $Re = 1, Ha = 1, \phi = 0.06$ and $\Pr = 6.2$.

	$V(y)$			$U(y)$		
η	**NM**	**HPM**	**%Error**	**NM**	**HPM**	**%Error**
0	0	0	0	1	1	9.99201E-14
0.1	0.031536	0.031536	3.94231E-07	0.811214	0.810273	0.004312136
0.2	0.114879	0.114879	7.31117E-09	0.642786	0.640942	0.010666076
0.3	0.234148	0.234148	6.406E-08	0.497688	0.495028	0.019876212
0.4	0.374868	0.374868	9.01469E-08	0.376093	0.372762	0.032934072
0.5	0.523888	0.523888	1.18899E-07	0.276303	0.272514	0.050985265
0.6	0.669183	0.669183	9.38714E-08	0.195535	0.191575	0.075286883
0.7	0.799622	0.799622	2.96393E-07	0.130546	0.126783	0.107182537
0.8	0.904758	0.904758	1.746E-07	0.07812	0.075006	0.148190076
0.9	0.974688	0.974688	2.24162E-07	0.035383	0.033476	0.200316815
1	1	1	0	0	0	0

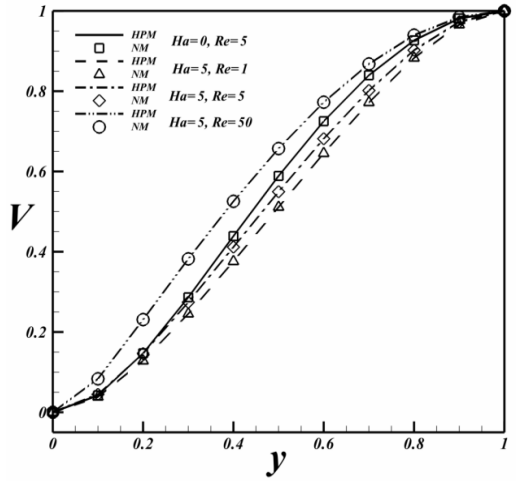

(a) $Ha = 0$

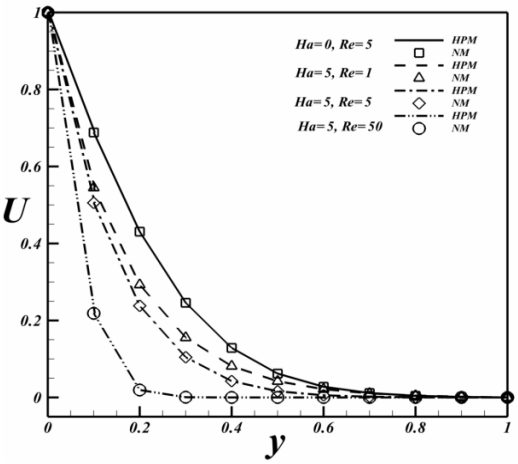

(b) $Ha = 5$

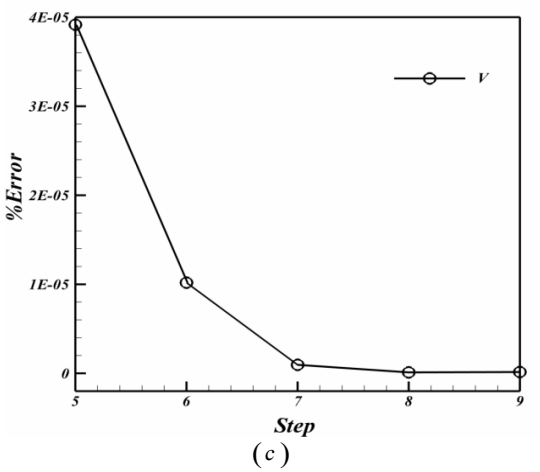

(c)

Figure 2. Comparison between the Numerical results and HPM solution for different values of active parameters when $\phi = 0.06$;(c) %Error for $\theta(\eta)$ (a) for different steps of HPM for $\phi = 0.06, Ha = 1, Re = 1$

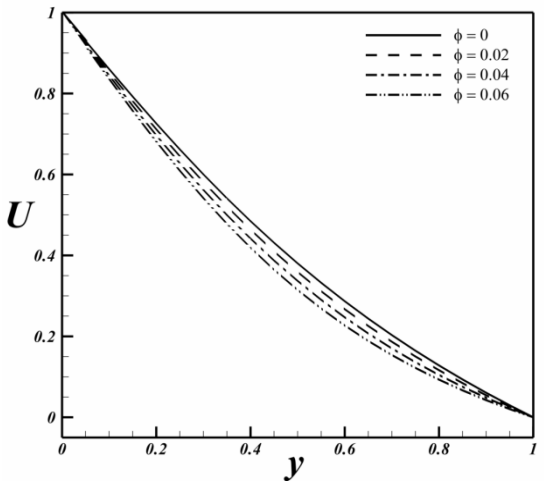

$Ha = 0$

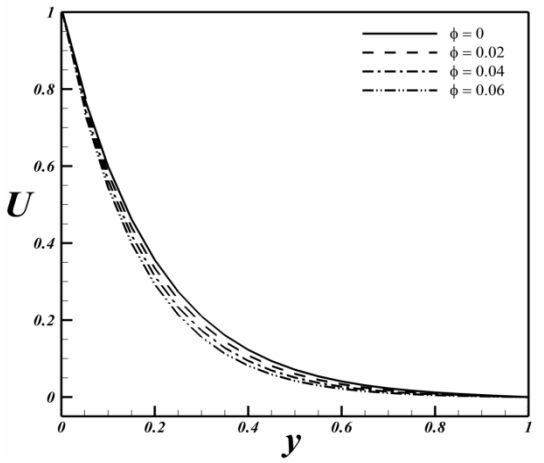

$Ha = 5$

Figure 3. Effect of nanoparticle volume fraction (ϕ), on $U(y)$, when $Re = 1$.

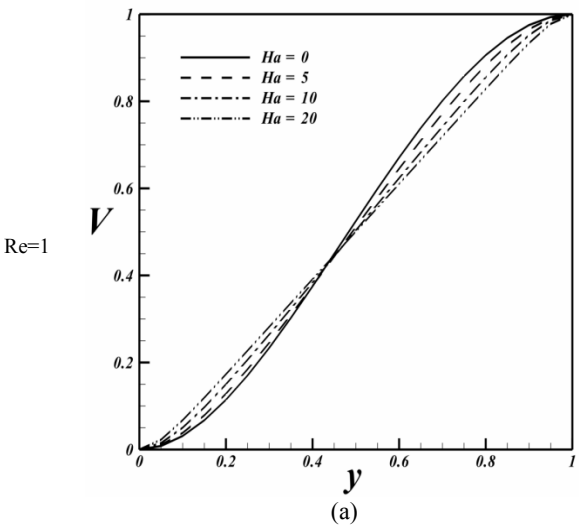

Re=1

(a)

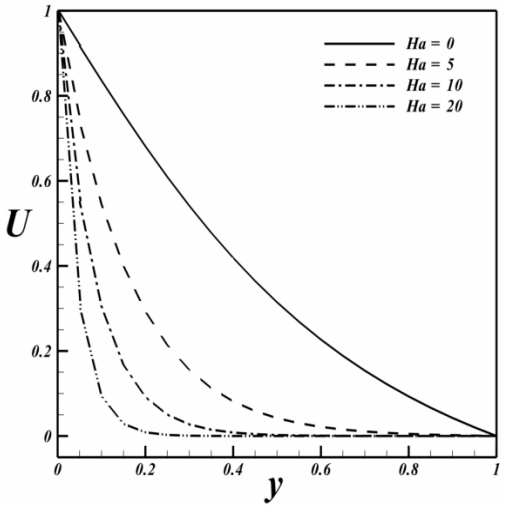

Re=1

(b)

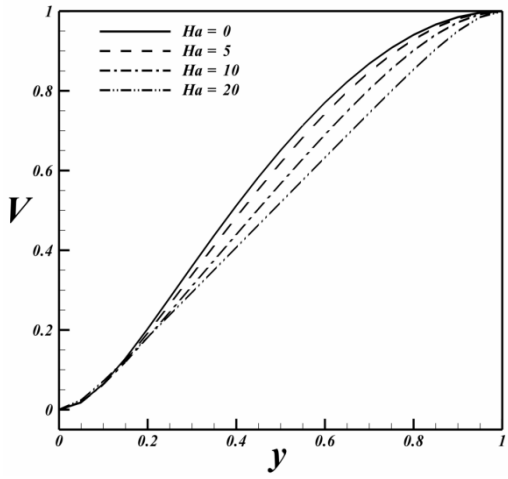

Re=20

(c)

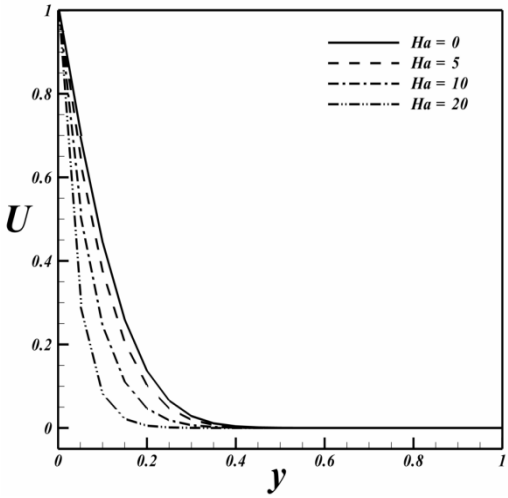

Re=20

(d)

Figure 4. Effect of various values of Hartmann numbers (Ha) on $V(y)$ and $U(y)$, when $\phi = 0.06$.

Figure 5 shows the effect of Reynolds number on $V(y)$ and $U(y)$ profiles at constant Hartmann number. It is worth to mention that the Reynolds number indicates the relative significance of the inertia effect compared to the viscous effect.

Thus, velocity profile decreases as *Re* increases and in turn increasing Re leads to increase in the magnitude of the skin friction coefficient. By increasing Reynolds number, $V(y)$ and $U(y)$ increase. These effects become less at higher Hartmann numbers. Also, it shows that increasing Hartmann number leads to increasing the curve of velocity profile.

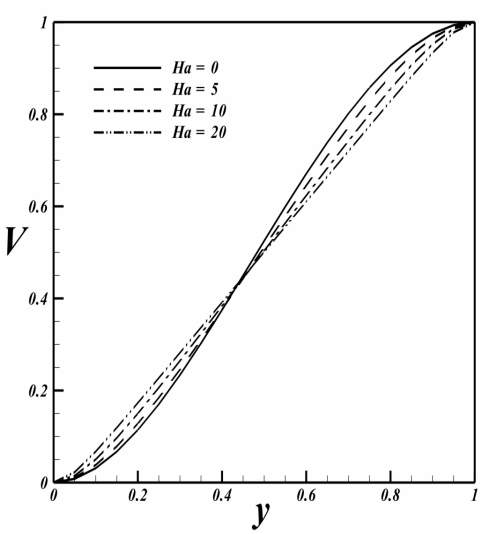

(a)

Ha=0

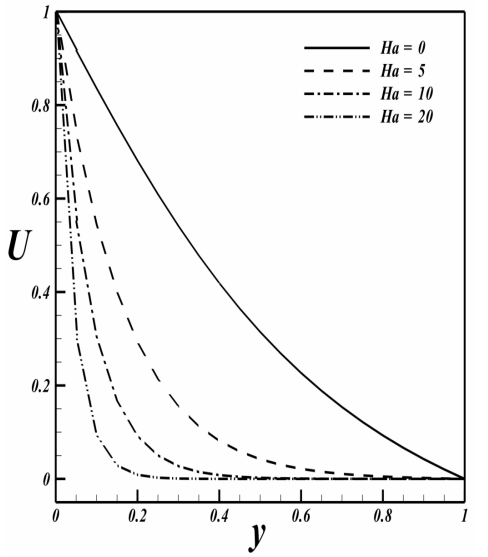

(b)

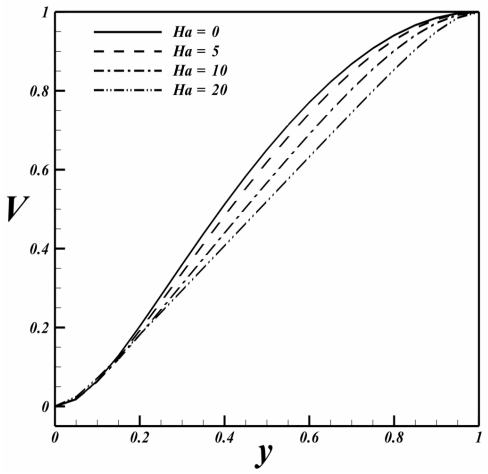

(c)

Ha=10

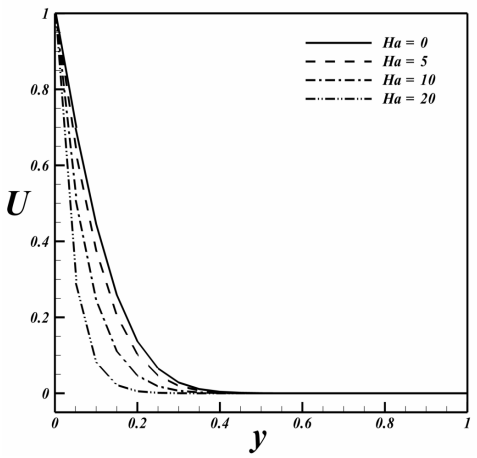

(d)

Figure 5. Effects of various values of Reynolds numbers on $V(y)$ and $U(y)$ when $\phi = 0.06$.

6. CONCLUDING REMARKS

The main aim of this paper is solving the problem of laminar nanofluid flow in a semi-porous channel in the presence of uniform magnetic field by homotopy perturbation method. It was found that HPM is a powerful approach. Also, as it is shown in the figures that there is a good agreement between the results of the present work and numerical data. The results indicate that velocity boundary layer thickness decreases with increasing Reynolds number and nanoparticle volume friction and it increases while Hartmann number increases. Furthermore, it can be seen that for low Reynolds numbers, as Hartmann number increases $V(y)$ decreases for $y > y_m$ but in opposite trend, it is observed for $y > y_m$. Whilst y_m is a meeting point that all curves joint together at this point. When Reynolds number increases this meeting point shifts to the solid wall and it can be seen that $V(y)$ decreases with increase of Hartmann number.

7. REFERENCES

1. Wernert, V., Schaf, O., Ghobarkar, H. and Denoyel, R., "Adsorption properties of zeolites for artificial kidney applications", ***Microporous and Mesoporous Materials***, Vol. 83, No. 1, (2005), 101-113.
2. Jafari, A., Zamankhan, P., Mousavi, S. and Kolari, P., "Numerical investigation of blood flow. Part ii: In capillaries", ***Communications in Nonlinear Science and Numerical Simulation***, Vol. 14, No. 4, (2009), 1396-1402.
3. R Goerke, A., Leung, J. and R Wickramasinghe, S., "Mass and momentum transfer in blood oxygenators", ***Chemical Engineering Science***, Vol. 57, No. 11, (2002), 2035-2046.
4. Mneina, S. S. and Martens, G. O., "Linear phase matched filter design with causal real symmetric impulse response", ***AEU-International Journal of Electronics and Communications***, Vol. 63, No. 2, (2009), 83-91.
5. Andoh, Y. and Lips, B., "Prediction of porous walls thermal protection by effusion or transpiration cooling. An analytical approach", ***Applied Thermal Engineering***, Vol. 23, No. 15, (2003), 1947-1958.
6. Runstedtler, A., "On the modified stefan–maxwell equation for isothermal multicomponent gaseous diffusion", ***Chemical Engineering Science***, Vol. 61, No. 15, (2006), 5021-5029.
7. Berman, A. S., "Laminar flow in channels with porous walls", ***Journal of Applied Physics***, Vol. 24, No. 9, (1953), 1232-1235.
8. Chandran, P., Sacheti, N. C. and Singh, A., "Hydromagnetic flow and heat transfer past a continuously moving porous boundary", ***International Communications in Heat and Mass Transfer***, Vol. 23, No. 6, (1996), 889-898.
9. He, J.-H., "Homotopy perturbation technique", ***Computer Methods in Applied Mechanics and Engineering***, Vol. 178, No. 3, (1999), 257-262.
10. He, J.-H., "Homotopy perturbation method: A new nonlinear analytical technique", ***Applied Mathematics and Computation***, Vol. 135, No. 1, (2003), 73-79.
11. Sheikholeslami, M., Ashorynejad, H., Ganji, D. and Kolahdooz, A., "Investigation of rotating mhd viscous flow and heat transfer between stretching and porous surfaces using analytical method", ***Mathematical Problems in Engineering***, Vol. 2011, No., (2011).
12. Sheikholeslami, M., Ashorynejad, H., Ganji, D. and Yıldırım, A., "Homotopy perturbation method for three-dimensional problem of condensation film on inclined rotating disk", ***Scientia Iranica***, (2012).
13. Hamad, M., Pop, I. and Md Ismail, A., "Magnetic field effects on free convection flow of a nanofluid past a vertical semi-infinite flat plate", ***Nonlinear Analysis: Real World Applications***, Vol. 12, No. 3, (2011), 1338-1346.
14. Soleimani, S., Sheikholeslami, M., Ganji, D. and Gorji-Bandpay, M., "Natural convection heat transfer in a nanofluid filled semi-annulus enclosure", ***International Communications in Heat and Mass Transfer***, Vol. 39, No. 4, (2012), 565-574.
15. Sheikholeslami, M., Ashorynejad, H., Domairry, G. and Hashim, I., "Flow and heat transfer of cu-water nanofluid between a stretching sheet and a porous surface in a rotating system", ***Journal of Applied Mathematics***, Vol. 2012, No., (2012).

16. Domairry, D., Sheikholeslami, M., Ashorynejad, H. R., Gorla, R. S. R. and Khani, M., "Natural convection flow of a non-newtonian nanofluid between two vertical flat plates", ***Proceedings of the Institution of Mechanical Engineers, Part N: Journal of Nanoengineering and Nanosystems***, Vol. 225, No. 3, (2011), 115-122.

17. Sheikholeslami, M., Gorji-Bandpay, M. and Ganji, D., "Magnetic field effects on natural convection around a horizontal circular cylinder inside a square enclosure filled with nanofluid", ***International Communications in Heat and Mass Transfer***, (2012).

18. Sheikholeslami, M., Soleimani, S., Gorji-Bandpy, M., Ganji, D. and Seyyedi, S., "Natural convection of nanofluids in an enclosure between a circular and a sinusoidal cylinder in the presence of magnetic field", ***International Communications in Heat and Mass Transfer***, (2012).

19. Sheikholeslami, M., Ganji, D., Ashorynejad, H. and Rokni, H. B., "Analytical investigation of jeffery-hamel flow with high magnetic field and nanoparticle by adomian decomposition method", ***Applied Mathematics and Mechanics***, Vol. 33, No. 1, (2012), 25-36.

20. Brinkman, H., "The viscosity of concentrated suspensions and solutions", ***The Journal of Chemical Physics***, Vol. 20, (1952), 571.

21. Desseaux, A., "Influence of a magnetic field over a laminar viscous flow in a semi-porous channel", ***International Journal of Engineering Science***, Vol. 37, No. 14, (1999), 1781-1794.

Nanofluid Flow in a Semi-porous Channel in the Presence of Uniform Magnetic Field

M. Sheikholeslami [a], D. D. Ganji [a], H. B. Rokni [b]

[a] *Department of Mechanical Engineering, Babol University of Technology, Babol, Iran*
[b] *University of Denver, Mechanical and Materials Engineering, 2390 S York St., Denver, CO 80208, USA*

P A P E R I N F O

Paper history:
Received 19 August 2012
Received in revised form 25 August 2012
Accepted 24 January 2013

Keywords:
Nanofluid
Laminar Flow
Semi-porous Channel
Uniform Magnetic
Homotopy Perturbation Method (HPM)

چکیده

در این مقاله مسئله‌ی جریان نانوسیال با لایه‌های نازک در کانال شبه متخلخل به وسیله‌ی روش آشفتگی هوموتوپی به صورت تحلیلی بررسی شده است. این مسئله در حضور ناحیه‌ی مغناطیسی متقاطع می‌باشد. در این‌جا تلاش شده است تا توانایی و کاربرد های وسیع روش آشفتگی هوموتوپی در مقایسه با روش عددی در حل مسائلی از این دست نشان داده شود. سیال مورد نظرآب حاوی مس به عنوان نانوذره است. رسانایی گرمایی موثر و گران‌روی نانوسیال به وسیله‌ی ماکسول–گانتس و مدل‌های برینکمن محاسبه شده‌اند. جواب‌های به دست آمده در مقایسه با خروجی‌های روش‌های عددی دقت قابل توجهی را نشان میدهد. نتیجه‌ی مشخصی که از نتایج روش عددی عرضه می‌شود این است که روش ذکر شده برای معادله‌های دیفرانسیلی غیرخطی راه حل‌هایی با دقت بالا فراهم می‌کند.بنا براین، اثر اعداد بی‌بعد را بررسی می‌کنیم: اصطکاک حجمی نانوسیال، عدد هارتمن برای نمایش نیروهای مغناطیسی و عدد رینولدز برای نیروهای دینامیکی. نتیجه گیریبحث در انتهای این بررسی آمده است.

doi: *10.5829/idosi.ije.2013.26.06c.10*